World Applied Sciences Journal 9 (8): 834-847, 2010
ISSN 1818-4952

Investigation of CO_2 Absorption in Hollow Fiber Membrane with Experimental and Simulation Methods

Sadegh Moradi

Department of Chemical Engineering Arak University, Arak, Iran

Abstract: The removal of carbon dioxide from gas mixtures is very important for greenhouse gas emission control. This study deals with the preparation and simulation of hollow fiber membrane made from polypropylene (PP) for CO_2 absorption. Polypropylene hollow fibers were prepared by melt-spinning method at speed of 100 m/min. Hollow fibers were obtained with the following typical geometries: outer diameter, 600 μm; inner diameter, 400 μm; length, 20 cm. To evaluate the hollow fibers performance as a membrane contactor, the simulation was performed for CO_2 absorption by the liquid absorbents. Both of physical and chemical absorption were considered in the simulations. Simulation results indicated that the hollow fiber membrane contactors have a great potential in the area of CO_2 absorption. Furthermore, polypropylene was shown to be a good membrane material for CO_2 absorption.

Key words: Hollow fiber membrane · Melt-spinning · Carbon dioxide · Gas absorption · Simulation

INTRODUCTION

Global expansion of industrial activities over the past three decades has caused the concentration of greenhouse gases to rise significantly in the atmosphere. This has contributed to global warming, which in turn has resulted in serious environmental problems [1]. Carbon dioxide is representing about 80% of greenhouse gases. It is reported that half of the CO_2 emissions are produced by industry and power plants using fossil fuels [2]. From the global environmental perspective, it is important to capture CO_2 to avert the threat of global warming, thereby attaining the carbon emission reduction targets set out by the Kyoto Agreement. Additionally, the CO_2 concentrations are typically 3-5% in gas-fired power plants and 13-15% in coal plants [3].

Current carbon dioxide capture technologies are based on a variety of physical and chemical processes including, absorption, adsorption, cryogenic and membrane techniques. Conventional processes for the removal of CO_2 suffer from many problems such as flooding, foaming, entraining, channeling, and high capital and operating costs. Therefore, many researchers have examined the possibilities of enhancing the efficiency of these processes to reduce the effect of their problems. Hollow fiber membrane contactors are expected to overcome the disadvantages of the conventional equipment when incorporated into the gas treating processes [4]. The characteristic of hollow fiber membrane contactors is that the gas stream flows on one side and the absorbent liquid flows on the other side of the membrane without phase dispersion, thus avoiding the problems often encountered in the conventional equipment such as flooding, foaming, channeling and entrainment.

Hollow fiber membranes are the most advantageous from of membranes used in the processes of gas separation. They can be produced by any method employed for the manufacture of chemical fibers, i.e. they can be spun from melt or half-melt or from a polymer solution. Melt-spinning is most economic method of hollow fiber membrane production. It is also a very ecological method, since no wastewater or harmful by-products are involved. Of all the thermoplastic polymers which can be processed by melt spinning, polyolefines have been found most suitable for making hollow fiber membranes [5] .One polymer of this group, polypropylene (PP), shows particularly desirable gas permeation properties.

EXPERIMENTAL

Materials: The hollow fibers were formed from a melt of polypropylene (PP, Grade R60) supplied by Arak Petrochemical Complex (Iran) with a melt flow index of 3 g/min.

Corresponding Author: Sadegh Moradi, Department of Chemical Engineering Arak University, Arak, Iran

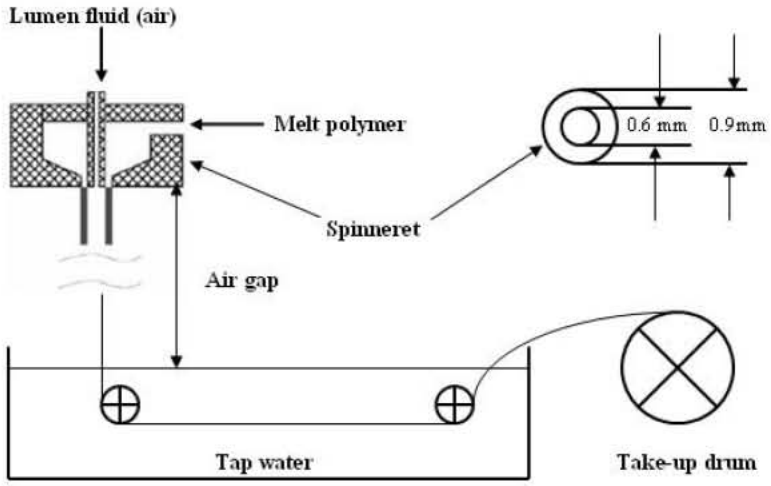

Fig. 1: Schematic drawing of melt-spinning apparatus

Fig. 2: Image of die which was used in spinning of hollow fibers

Hollow Fibers Preparation: The hollow fibers were extruded at high pressure through a die (a fine capillary) which was designed and fabricated for this work. The polymer was extruded into cooling water that both cools the fiber and exerts a drag force on the fiber. At some distance below the spinneret (a meter or more), a mechanical roll provides the force that drives the process. Fig. 1 shows a schematic diagram of a hollow fibers preparation apparatus. Dimensions of spinneret are shown in the Fig. 1. Fig. 2 shows image of die which was used in this work.

Table 1: Dimensions of hollow fiber melt-spun from polypropylene

Parameter	Value
Inner fiber diameter (μm)	400
Outer fiber diameter (μm)	600
Fiber length (cm)	20

Variables in the Spinning Process Were:

- Extrusion rate: 100 m/min;
- Output rate: 50 g/min;
- Melt temperature: 230°C;
- Sub-spinneret zone cooling conditions.

Stretching of hollow fibers was carried out at room temperature and at a draw ratio of 2.5. The dimensions of obtained hollow fibers are shown in Table 1.

Simulation of CO_2 Absorption in Hollow Fiber Membrane: To investigate the performance of hollow fibers as membrane contactor for gas absorption, a comprehensive two-dimensional mathematical model was used for the transport of carbon dioxide through hollow fiber membrane (HFM) contactors. In this work we study the separation of CO_2 from CO_2/N_2 gas mixture using amines and carbonate aqueous solutions as absorbents in hollow fiber membrane contactors. The model was based on "non-wetted mode" in which the gas mixture filled the membrane pores for countercurrent gas-liquid contacts. Laminar parabolic velocity profile was used for the gas flow in the tube side; whereas, the liquid flow in the shell side was characterized by Happel's free surface model. Axial and radial diffusion inside the fiber, through the membrane, and within the shell side of the contactor were considered in the model.

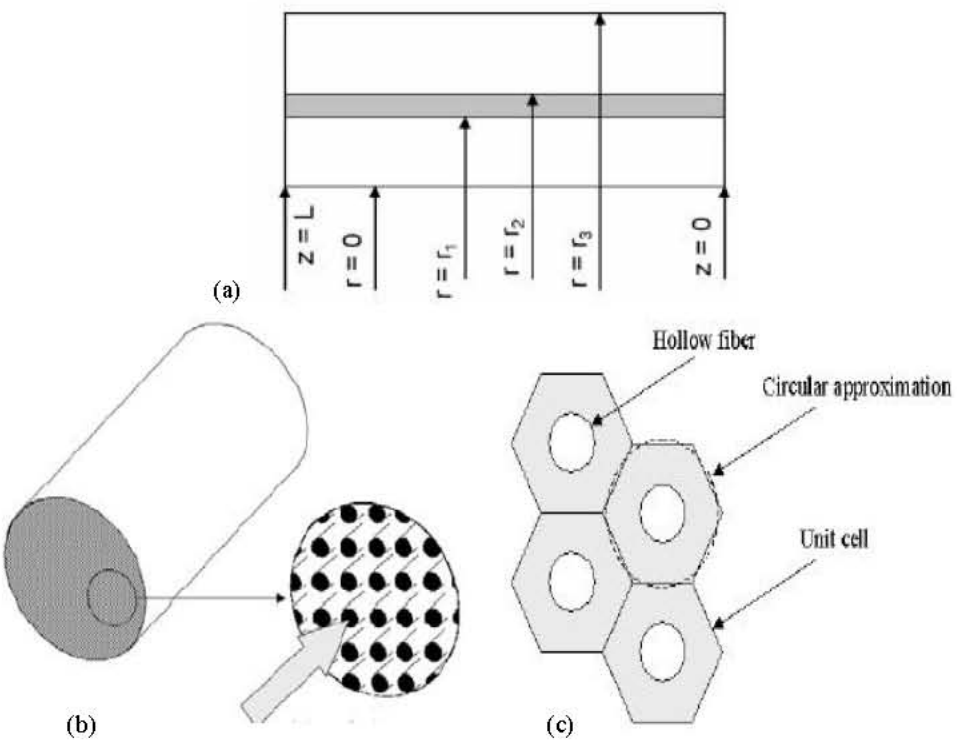

Fig. 3: (a) Model domain (b) A schematic diagram for the membrane contactor (c) Cross sectional area of the membrane contactor and circular approximation of portion of the fluid surrounding the fibers.

Formulation of Mass Transfer and Absorption: The model is used for a segment of a hollow fiber, as shown in Fig. 3b, through which the gas mixture flows with a fully developed laminar parabolic velocity profile. The fiber is surrounded by a laminar liquid flow in an opposite direction. Fig. 3c shows the cross sectional area of the membrane contactor. Based on Happel's free surface model [6], only portion of the fluid surrounding the fiber is considered which may be approximated as circular cross section. Therefore, the membrane contactor consists of three sections: tube side, membrane, and shell side. The steady state two-dimensional material balances are carried out for all three sections. The gas mixture is fed to the tube side (at $z = 0$), while the solvent is passed through the shell side (at $z = L$). CO_2 is removed from the gas mixture by diffusing through the membrane and then absorption and reaction with the solvent.

The used assumptions were: (1) steady state and isothermal conditions; (2) fully developed parabolic gas velocity profile in the hollow fiber; (3) ideal gas behavior is imposed; (4) the Henry's law is applicable for gas-liquid interface; (5) Laminar flow for gas and liquid flow in the contactor.

Tube Side: The continuity equation for each species in a reactive absorption system can be expressed as [7]:

$$\frac{\partial C_i}{\partial t} = -(\nabla \cdot C_i V) - (\nabla \cdot J_i) + R_i \quad (1)$$

Where C_i, J_i, R_i, V and t are the concentration, diffusive flux, reaction rate of species I, velocity and time, respectively. Either Fick's law of diffusion or Maxwell-Stefan theory can be used for the determination of diffusive fluxes of species i.

The continuity equation for steady state for CO_2 in the tube side of contactor for cylindrical coordinate is obtained using Fick's law of diffusion for the estimation of the diffusive flux:

$$D_{CO2-tube}\left[\frac{\partial^2 C_{CO2-tube}}{\partial r^2} + \frac{1}{r}\frac{\partial C_{CO2-tube}}{\partial r} + \frac{\partial^2 C_{CO2-tube}}{\partial z^2}\right] = V_{z-tube}\frac{\partial C_{CO2-tube}}{\partial z} \quad (2)$$

The velocity distribution in the tube is assumed to follow Newtonian laminar flow [7]:

$$V_{z-tube} = 2u\left[1-\left(\frac{r}{r_1}\right)^2\right] \quad (3)$$

Where u is average velocity in tube side.

Boundary Conditions:

$$\text{at } z = 0,\ C_{CO2\text{-}tube} = C_0,\ C_{absorbent} = 0 \quad (4)$$

$$\text{at } r = r_1,\ C_{CO2\text{-}tube} = C_{CO2\text{-}membrane} \quad (5)$$

$$\text{at } r = 0,\ \frac{\partial C_{CO2-tube}}{\partial r} = 0 \ \text{(symmetry)} \quad (6)$$

Membrane: The steady-state continuity equation for the transport of CO_2 inside the membrane, which is considered to be due to diffusion alone, may be written as:

$$D_{CO2-membrane}\left[\frac{\partial^2 C_{CO2-membrane}}{\partial r^2}+\frac{1}{r}\frac{\partial C_{CO2-membrane}}{\partial r}+\frac{\partial^2 C_{CO2-membrane}}{\partial z^2}\right]=0 \quad (7)$$

Boundary Conditions Are Given As:

$$\text{at } r = r_1,\ C_{CO2\text{-}membrane} = C_{CO2\text{-}tube} \quad (8)$$

$$\text{at } r = r_2,\ C_{CO2\text{-}membrane} = C_{CO2\text{-}shell}/m \quad (9)$$

Where m is the physical solubility of CO_2 in the solution.

Shell Side: The steady-state continuity equation for the transport with chemical reaction of CO_2 and potassium carbonate in the shell side, where CO_2 is absorbed and reacts with solvent may be written as:

$$D_{i-shell}\left[\frac{\partial^2 C_{i-shell}}{\partial r^2}+\frac{1}{r}\frac{\partial C_{i-shell}}{\partial r}+\frac{\partial^2 C_{i-shell}}{\partial z^2}\right]=V_{z-shell}\frac{\partial C_{i-shell}}{\partial z}-R_i \quad (10)$$

It is suggested that Happel's free surface model can be used to characterize the out fibers velocity profile [6]. Although the flow in the real hollow fiber module is not absolutely according with Happel's model, Happel's model has been extensively used for the membrane contactors. The laminar parabolic velocity profile in the outside of fibers is:

$$V_{z-shell} = 2u\left[1-\left(\frac{r_2}{r_3}\right)^2\right]\times\frac{(r/r_3)^2-(r_2/r_3)^2+2\ln(r_2/r)}{3+(r_2/r_3)^4-4(r_2/r_3)^2+4\ln(r_2/r_3)} \quad (11)$$

Where u, r_3, r_2 represent the average velocity, radius of free surface (Fig. 3a) and fiber outer radius, respectively. r_3 can be defined as:

$$r_3 = \left(\frac{1}{1-\phi}\right)^{1/2} r_2 \quad (12)$$

in which ϕ is the volume fraction of the void. It can be calculated as follows:

$$1\text{-}\phi = \frac{n r_2^2}{R^2} \quad (13)$$

Where n is the number of fibers and R is the module inner radius.

Boundary Conditions for Shell Side Are Given As:

$$\text{at } z = L,\ C_{CO2\text{-}shell} = 0,\ C_{absorbent} = C_{in} \quad (14)$$

$$\text{at } r = r_3,\ \frac{\partial C_{i-shell}}{\partial r} = 0 \ \text{(insulation)} \quad (15)$$

$$\text{at } r = r_2,\ C_{CO2\text{-}shell} = C_{CO2\text{-}membrane}\cdot m,\ \frac{\partial C_{absorbent-shell}}{\partial r} = 0 \quad (16)$$

Reaction Rate for CO_2 Absorption into Amine Aqueous Solutions: Two typical amine solution of monoethanolamine (MEA) and methyldiethanol amine (MDEA) were used as absorbent in this study. The zwitterions-mechanism was adopted for the reaction of CO_2 with primary or secondary alkanolamines [8]:

$$CO_2 + R_1R_2NH \xleftrightarrow{k_1} R_1R_2NH^+COO^- \quad (17)$$

$$R_1R_2NH^+COO^- + B \xrightarrow{k_b} R_1R_2NCOO^- + BH^+ \quad (18)$$

Where R_1 is an alkyl and R_2 is H for primary amines and an alkyl for secondary amines, B is a base that could be an amine, OH, or H_2O. For this mechanism, the reaction rate of CO_2 with MEA can be expressed as follow [9]:

$$R_{CO2-MEA} = \frac{k_{1,MEA}C_{CO2}C_{MEA}}{1+\dfrac{k_{-1}}{k_{H2O}C_{H2O}+k_{OH^-1}C_{OH^-1}+k_{MEA}C_{MEA}+k_{MDEA}C_{MDEA}}} \quad (19)$$

The reaction kinetics for the reaction of CO_2 with MDEA aqueous has been studied extensively. All the data for CO_2 with MDEA are in agreement well with the pseudo-first- order reaction as follow [8, 11]:

Table 2: Parameters used in simulation for CO_2 absorption into amines aqueous solutions

Parameter	value
$D_{CO2/N2}$ (25°C, 121.3 kPa)	1.39×10^{-5} m^2s^{-1} [12]
$D_{CO2/MDEA}$ (25°C, 10 wt. % MDEA)	1.63×10^{-9} m^2s^{-1} [13]
$D_{MDEA/Solution}$ (25°C, 10 wt. % MDEA)	6.91×10^{-10} m^2s^{-1} [14]
$D_{MEA/Solution}$ (25°C, 10 wt. % MDEA)	1.09×10^{-10} m^2s^{-1} [14]
$D_{CO2/Membrane}$(25°C, 1atm)	3.38×10^{-6} [7]
x_w	$10^{-22.795+0.0294T}$ [11]
x_p	$10^{-14.123+0.01842T}$ [11]
$k_{2,MDEA}$	1.34×10^{6} exp (-5771/T) m^3mol^{-1} s^{-1} [10]
$k_{1,MEA}$	7.973×10^{9} exp (-6243/T) m^3mol^{-1} s^{-1} [11]
k_{OH^-}	$10^{13.625-2895/T}$ m^3 $kmol^{-1}$ s^{-1} [11]
$k_{1,MEA}k_{H2O}/k_{-1}$	1.1 exp (-3472/T) $m^6mol^{-2}s^{-1}$ [11]
$k_{1,MEA}k_{MEA}/k_{-1}$	1.563×10^{8} exp (-7544/T) $m^6mol^{-2}s^{-1}$ [11]
$k_{1,MEA}k_{MDEA}/k_{-1}$	86.76 exp (-3637/T) $m^6mol^{-2}s^{-1}$ [11]
Henry constant of CO_2 with aqueous (25 °C, 10% MDEA)	0.891 [14]

$$R_{CO2-MDEA} = k_{2,MDEA}C_{CO2}C_{MDEA} \quad (20)$$

The reaction kinetics for the reaction of CO_2 with H_2O can be expressed as follow [8]:

$$R = R_{CO2-OH^-} + R_{CO2-H2O} \quad (21)$$

The reaction of CO_2 with H_2O can be negligible due to the weak contribution [8].

The reaction of CO_2 with hydroxyl ion can be described as [10]:

$$R_{CO2-OH^-} = k_{OH^-}C_{CO2}C_{OH^-} \quad (22)$$

$$C_{OH^-} = \frac{x_w}{x_p}\left(\frac{1-\alpha}{\alpha}\right) \quad \alpha \geq 10^{-3} \quad (23)$$

$$C_{OH^-} = \sqrt{\frac{x_w}{x_p}C_{amine}}, \quad \alpha < 10^{-3} \quad (24)$$

Where α is the CO_2 loading in amine solution. The value of x_w and x_p is given in Table 2.

Reaction Rate for CO_2 Absorption into K_2CO_3 Aqueous Solution: Absorption of carbon dioxide into the aqueous carbonate solutions has been studied by many investigators [15-17]. In these studies most of the work has been carried out using high bicarbonate to the carbonate ratios. In such cases the carbon dioxide into the aqueous carbonate buffer solutions can be treated as absorption accompanied by an irreversible pseudo-first order reaction. The chemical absorption mechanism under the conditions of low or negligible bicarbonate to carbonate ratio is, however, more complex and contains two-step reversible reactions [18].

When the potassium carbonate is dissolved in water it is ionized into the potassium ion (K^+) and carbonate ion (CO_3^{2-}). The bicarbonate ion (HCO_3^-) and hydroxyl ion (OH^-) are then generated by the inverse of reaction 26 in following reaction scheme. The various reactions taking place during the absorption of carbon dioxide into the aqueous potassium carbonate solution are given below [15].

$$CO_2 + OH^- \xleftrightarrow{k_{25}} HCO_3^- \quad (25)$$

$$HCO_3^- + OH^- \xleftrightarrow{k_{26}} CO_3^{2-} + H_2O \quad (26)$$

$$2H_2O \xleftrightarrow{k_{27}} H_3O^+ + OH^- \quad (27)$$

$$CO_2 + 2H_2O \xleftrightarrow{k_{28}} HCO_3^- + H_3O^+ \quad (28)$$

$$CO_2 + CO_3^{2-} + H_2O \longleftrightarrow 2HCO_3^- \quad (29)$$

Reactions (25) and (28) are rate controlling reactions [15, 16]. Reaction (25) is practically irreversible for the pH values greater than 10. Reaction (28) is much slower and only of importance in solutions with pH values less than 8 [19]. The reactions (26) and (27) involve only proton transfer and can be considered as instantaneous so that they can be assumed to be at equilibrium [15]. Reaction (29) is the overall reaction of carbon dioxide absorption in aqueous carbonate solution. The corresponding equilibrium constants of the reactions are defined as follows:

$$K_1 = \frac{[HCO_3^-]}{[CO_2][OH^-]} \quad (30)$$

$$K_2 = \frac{[CO_3^{2-}]}{[HCO_3^-][OH^-]} \quad (31)$$

$$K_w = [H_3O^+][OH^-] \quad (32)$$

$$K_4 = \frac{[HCO_3^-][H_3O^+]}{[CO_2]} \quad (33)$$

All the kinetic parameters can be obtained from the literature and are given in Appendix A.

The dimensionless model equations related to tube, membrane and shell side with the appropriate boundary conditions were solved using COMSOL software, which uses finite element method (FEM) for numerical solutions of differential equations. The finite element analysis is combined with adaptive meshing and error control using a variety of numerical solvers such as DASPK. This solver is an implicit time-stepping scheme, which is well suited for solving stiff and non-stiff non-linear boundary value problems. We used an IBM-PC-Pentium4 (CPU speed is 2800 MHz) to solve the set of equations. The computational time for solving the set of equations was 35 minutes.

RESULTS AND DISCUSSION

CO_2 Absorption into Amine Aqueous Solutions

Concentration Distribution of CO_2 in the Contactor: Fig. 4 presents the concentration distribution of CO_2 in the tube, membrane and shell side of the contactor. The gas mixture flows from one side of the contactor ($z = 0$) where the concentration of CO_2 is the highest (C_0), whereas the solvent (MDEA) flows from the other side ($z = L$) where the concentration of CO_2 is assumed to be zero. As the gas flows through the tube side, it moves to the membrane due to the concentration difference and then it is absorbed by the moving solvent.

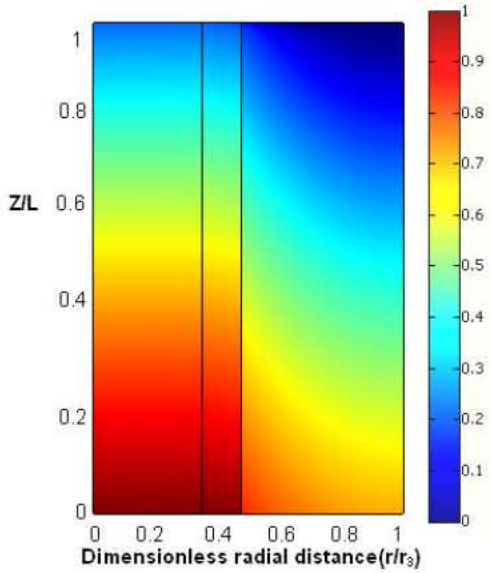

Fig. 4: A representation of the concentration distribution of CO_2 (C/C_0) in the membrane contactor for the absorption of CO_2 in MDEA. Gas flow rate= liquid flow rate = 100 ml/min; CO_2 inlet concentration = 10% vol.; amine (MDEA) inlet concentration = 10% wt; n=100; R=0.5 cm.

Effect of Liquid Flow Rate on the Absorption of CO_2: The percentage removal of CO_2 can be calculated from the equation below:

$$\%\ \text{removal}\ CO_2 = 100\frac{(v\times C)_{inlet} - (v\times C)_{Outlet}}{(v\times C)_{inlet}} = 100\left(1 - \frac{C_{outlet}}{C_{inlet}}\right) \quad (34)$$

Where v and C are the volumetric flow rate and concentration, respectively. C_{outlet} is calculated by integrating the local concentration at outlet of tube side ($z = L$):

$$C_{outlet} = \frac{\iint_{Z=L} C(r)dA}{\iint_{Z=L} dA} \quad (35)$$

The change in volumetric flow rate is assumed to be negligible and thus % CO_2 removal can be approximated by Eq. (34).

In Fig. 5, the CO_2 outlet concentration in gas is plotted as a function of absorbent flow rate or velocity for several absorbents and Fig. 6 illustrates the variation of the fractional removal of CO_2 as a function of liquid flow rate or velocity. As the absorbent flow rate increases, the transfer rate of carbon dioxide into the liquid increases because the concentration gradients of CO_2 and absorbent in the liquid increase, thus the CO_2 outlet concentration in gas decreases (Fig. 5) and the fractional removal of CO_2 increases (Fig. 6).

The behavior of CO_2 absorbed in MDEA/MEA mixed amines with different composition also illustrated in Figs. 5 and 6. Adding a little of MEA into MDEA aqueous solution, the capture of CO_2 increases. This is not surprise because the reaction rate constant of MEA with CO_2 is much higher than that of MDEA with CO_2. The transfer rate of carbon dioxide into the liquid increases as the concentration of MEA in mixed amines increases. As a result, the CO_2 outlet concentration in gas decreases and the fractional removal of CO_2 increases with increasing concentration of MEA in MDEA/MEA aqueous solution.

Fig. 7 shows the dimensionless concentration of amines versus dimensionless axial distance. The numerical results clearly show the concentrations of amines decrease as the axial increases. Also it can be seen the differences of dimensionless concentration of MEA is much larger than that of MDEA. This indicates the concentration gradient of MEA is much larger than that of MDEA due to the larger reaction coefficient of MEA with CO_2. Thus the diffuse flux of MEA is higher than that of MDEA in hollow fiber membrane. Consequentially, the consumption of MEA is larger than that of MDEA.

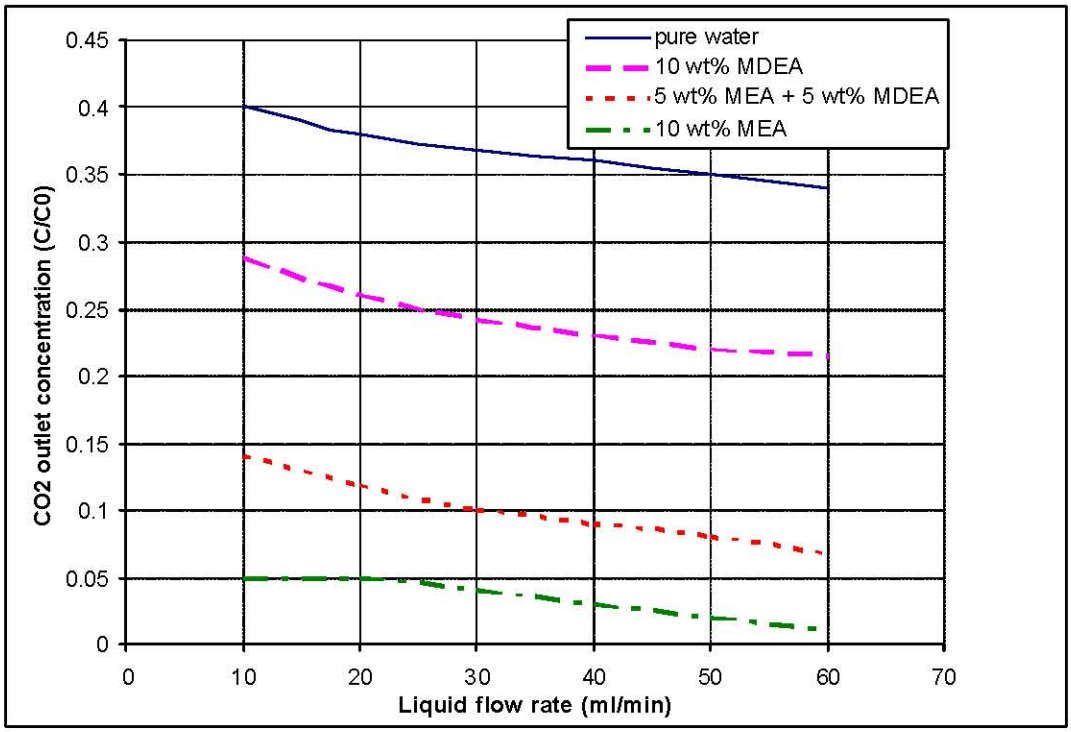

Fig. 5: Relationship between CO_2 outlet concentration in gas and liquid flow rate for various amines. Gas pressure= 121.3 kPa; temperature= 298 K; n=100; R=0.5 cm; Gas flow rate=100 ml/min.

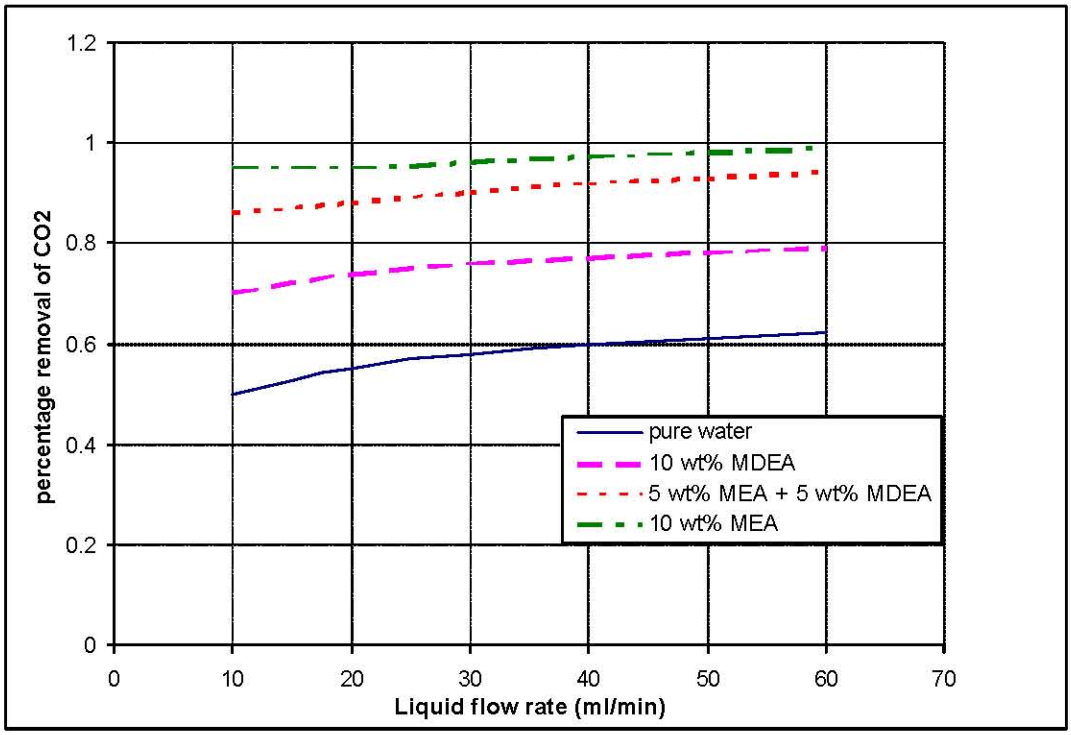

Fig. 6: Relationship between percentage removal CO_2 and liquid flow rate for various amines. Gas pressure= 121.3 kPa; temperature= 298 K; n=100; R=0.5 cm; Gas flow rate= 100 ml/min.

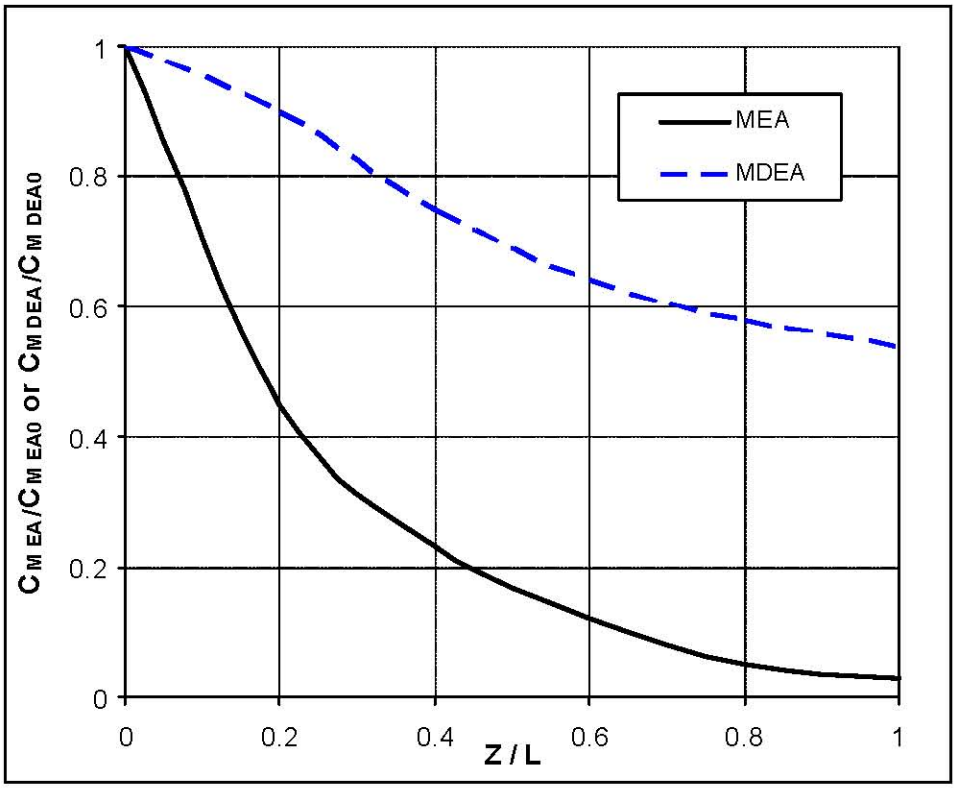

Fig. 7: Dimensionless concentration of amines vs. dimensionless axial distance. Gas pressure =121.3 kPa; temperature= 298 K; n=100; R=0.5 cm; Gas flow rate=liquid flow rate=50 ml/min; r/r_3 = 0.8.

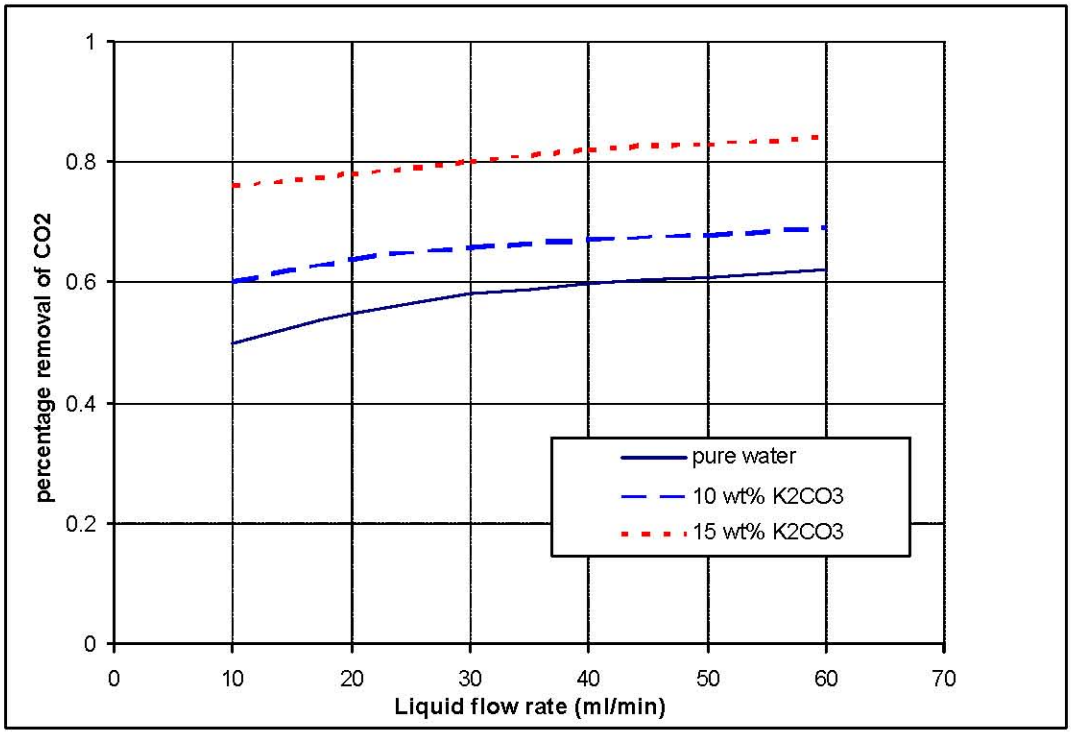

Fig. 8: Effect of liquid flow rate on the percentage removal of CO_2 for the absorption of CO_2 in K_2CO_3. Gas pressure= 121.3 kPa; temperature= 298 K; n=100; R=0.5 cm; Gas flow rate= 100 ml/min.

CO_2 Absorption into K_2CO_3 Aqueous Solution: Fig. 8 shows the percentage removal of CO_2 as a function of liquid flow rate through the fibers for a constant gas inlet flow rate. It can be seen from the figure that as the liquid velocity increases the gas outlet concentration of carbon dioxide decreases. This indicates the increase in the removal rate of carbon dioxide with the liquid flow rate. As expected, the carbon dioxide concentration decreases as the liquid flow rate increases. The effect of the concentration of carbonate solution is also shown in the figure. It can be seen from the figure that as the concentration of the carbonate solution is increased, the concentration of the absorbed carbon dioxide is also increased. This indicates that the increase in the concentration of carbonate ions results into the increase in carbon dioxide absorption.

It can be seen from the figure that the absorption is a strong function of the liquid velocity when the liquid velocity is relatively low. However, at higher velocities the absorption is less dependent on the liquid velocity. It is known from the theory of mass transfer with chemical reaction that in the case of fast reaction regime the absorption flux is independent of the mass transfer coefficient whereas in the case of instantaneous reaction regime the absorption flux depends on the mass transfer coefficient. In the present case of gas absorption accompanied with chemical reaction into a liquid flowing through hollow fiber, there is relatively less depletion of the reactive species at the gas-liquid interface over the entire length of fiber at higher liquid velocities. This situation resembles to the fast reaction regime. Therefore in this case the absorption rate is dominated by the chemical reaction rate and the liquid velocity has less influence on the average absorption flux. However, at lower velocities significant depletion of the reactive species may occur. For extreme case of the complete depletion of the reactive species at the interface, the reaction regime may change from fast reaction regime at the liquid inlet to instantaneous reaction regime at liquid exit. In such cases the absorption rate is limited by the radial diffusion of reacting species to the reaction plane and the flux is strongly influenced by the mass transfer coefficient and hence by the liquid velocity.

The figures show absorption of carbon dioxide in amines aqueous solutions is higher than that in carbonate solution because the reaction rate and solubility of carbon dioxide in amines aqueous solutions is greater than carbonate solution that increases both physical and chemical absorption of carbon dioxide in amines.

CONCLUSION

Absorption of CO_2 in hollow fiber membrane contactors was studied in this work. Polypropylene hollow fibers were prepared by melt-spinning process. Simulation was performed for hollow fibers as membrane contactor to study performance of hollow fibers in gas absorption process. A mathematical model was used to describe absorption of CO_2 in the contactor. The model was based on solving the conservation equations for three sections of contactor. The finite element method (FEM) was used to solve the differential equations. Absorption of CO_2 in amines and carbonate aqueous solutions was simulated in this work. The amines aqueous solutions (MDEA and MEA) were better for absorption of CO_2 because of high solubility and reaction rate of CO_2 with amines. The simulation results for the absorption of CO_2 in liquid solvents indicated that the removal of CO_2 increased with increasing liquid velocity in the shell side. The polypropylene (PP) hollow fiber membrane contactor was found to be very efficient in purification of gas streams.

The results in this work show that the detailed numerical model developed is able to predict the performance of the membrane contactors. The numerical simulation can take into account complex chemical reaction schemes. Thus the model can be used to predict the mass transfer performance of the hollow fiber gas-liquid membrane contactor for other reactive as well as non-reactive systems simply by changing the physical and kinetic parameters. Furthermore, the model also represents a design and optimization tool for multi-component membrane gas absorption processes using membrane modules.

ACKNOWLEDGMENTS

The authors would like to thank Arak University for the financial support. In addition, the authors would like to thank Dr. Miri, Birmingham University, for supplying the COMSOL software.

Nomenclature

A	Cross section of tube (m^2)
C_0	inlet CO_2 concentration (mol/m^3)
C	concentration (mol/m^3)
$C_{CO2\text{-}membrane}$	CO_2 concentration in the membrane (mol/m^3)
$C_{CO2\text{-}shell}$	CO_2 concentration in the shell (mol/m^3)
$C_{CO2\text{-}tube}$	CO_2 concentration in the tube (mol/m^3)

C_i	Concentration of any species (mol/m^3)
$C_{i\text{-}shell}$	Concentration of any species in the shell (m^2/s)
C_{in}	Absorbent concentration at the inlet (mol/m^3)
C_{inlet}	Inlet concentration of CO in the tube (mol/m^3)
C_{outlet}	Outlet concentration of CO_2 in the tube (mol/m^3)
D	diffusion coefficient (m^2/s)
$D_{CO2\text{-}membrane}$	Diffusion coefficient of CO_2 in the membrane (m^2/s)
$D_{CO2\text{-}tube}$	Diffusion coefficient of CO_2 in the tube (m^2/s)
$D_{i\text{-}shell}$	Diffusion coefficient of any species in the shell (m^2/s)
J_i	Diffusive flux of any species (mol/m^2.s)
k	Reaction rate coefficient of CO_2 with absorbent (m^3 /mol.s)
K	Equilibrium constant
L	Length of the fiber (m)
m	Physical solubility (-)
n	Number of fibers
P	Pressure (Pa)
$r1$	Tube inner radius (m)
r_2	Tube outer radius (m)
$r3$	Inner shell radius (m)
r	Radial coordinate (m)
R	Module inner radius (m)
R_i	Overall reaction rate of any species (mol/m^3.s)
t	Time (s)
T	Temperature (K)
u	Average velocity (m/s)
V	Velocity in the module (m/s)
$Vz\text{-}shell$	Z-velocity in the shell (m/s)
$V_{z\text{-}tube}$	Z-velocity in the tube (m/s)
z	Axial coordinate (m)
Z	ionic charge (-)

Greek Symbols

v	Volumetric flow rate (m^3/s)
ϕ	Module volume fraction

Appendix A

Solubility: The distribution coefficient of CO_2 in pure water was taken from Versteeg and van Swaaij [20].

$$m_{w,CO2} = 3.59\times10^{-7} RT \exp\left(\frac{2044}{T}\right) \quad (A.1)$$

The solubility of gas in aqueous electrolytic solutions was estimated using the method presented by Weisenberger and Schumpe [21]. The distribution coefficient for CO_2 in aqueous solution of potassium carbonate was determined using Eqs. (A.2) and (A.3).

$$\log\left(\frac{m_{w,G}}{m_G}\right) = (0.0959 + h_G)[K^+] + (0.0839 + h_G)[OH^-] + (0.0967 + h_G)[HCO_3^-] + (0.1423 + h_G)[CO_3^{2-}] \quad (A.2)$$

Where the ionic concentrations are in kmolm^{-3}. h_G is the gas specific constant and is given for CO_2 in following equation:

$$h_G = -0.0172 - 3.38\times10^{-4}(T - 298.15) \quad (A.3)$$

A.2. Diffusivity: The diffusivity of CO_2 in pure water, $D_{w,CO2}$ was taken from Versteeg and van Swaaij [20].

$$D_{w,CO2} = 2.35\times10^{-6} \exp\left(\frac{-2119}{T}\right) \quad (A.4)$$

The diffusion coefficients of gases into aqueous electrolyte solutions were estimated by the method suggested by Ratcliff and Holdcroft [22].

$$\frac{D}{D_w} = 1 - (0.154[K_2CO_3] + 0.0723[KHCO_3]) \quad (A.5)$$

Where concentrations are in kmol m^{-3}.

A.3. Kinetic Rate Constants: An expression for the forward rate constant, k_{25}, as a function co-electrolytes concentration was presented by Pohorecki and Moniuk [23].

$$\log\frac{k_{25}}{k_{25}^{\infty}} = 0.22\left(0.5[K^+]Z^2_{K^+}\right) + 0.22\left(0.5[OH^-]Z^2_{OH^-}\right) + 0.085\left(0.5[CO_3^{2-}]Z^2_{CO_3^{-2}}\right) \quad (A.6)$$

Where k_{25}^{∞} (m^3 kmol^{-1} s^{-1}) is the rate constant for infinitely dilute solution.

$$\log k_{25}^{\infty} = 11.916 - \frac{2382}{T} \quad (A.7)$$

The effect of HCO_3^- on the value of k_{25} has not been reported, hence its influence on the forward rate constants was neglected.

Since the reactions (26) and (27) involve only proton transfer and can be considered as instantaneous, these reactions were assumed to be at equilibrium.

The reaction rate constant of the reaction of water with carbon dioxide, k_{28}, as a function of temperature is given by Sharma and Danckwerts [17]. The reaction is first order with respect to the concentration of the carbon dioxide.

$$k_{28} = 329.850 - 110.541 \log T - \frac{17265.4}{T} \quad \text{(A.8)}$$

A.4. Equilibrium Constants: The equilibrium constant of the reaction (25), K_1 (m^3 $kmol^{-1}$), can be determined by the combination of the equilibrium for reaction (28) and reaction (27). The equilibrium constant for the reaction (26), K_2 (m^3 $kmol^{-1}$), at infinite dilution is reported by Hikita *et al.* [15].

$$\log K_2^{\infty} = \frac{1568.94}{T} + 0.4134 - 0.006737T \quad \text{(A.9)}$$

The effect of the electrolyte concentration on K_2 is given by Hikita *et al.* [15] and Roberts and Danckwerts [16].

$$\log \frac{K_2}{K_2^{\infty}} = \frac{1.01\sqrt{[K^+]}}{1+1.49\sqrt{[K^+]}} + 0.061[K^+] \quad \text{(A.10)}$$

The solubility product, K_w ($kmol^2$ m^{-6}), was taken from Tsonopolous *et al.* [24].

$$\log K_w = -\left(\frac{5839.5}{T} + 22.4773 \log T - 61.2062\right) \quad \text{(A.11)}$$

The equilibrium constant of reaction (28), K_4 ($kmolm^{-3}$) is reported in Sharma and Danckwerts [17].

$$\log K_4 = \frac{-3404.7}{T} + 14.843 - 0.03279T \quad \text{(A.12)}$$

REFERENCES

1. Gabelman, A. and S.T. Hwang, 1999. Hollow fiber membrane contactors, J. Membr. Sci., 159: 61-106.
2 Herzog, H., B. Eliasson and O. Kaarstad, 2000. Capturing greenhouse gases, Sci. Am., 182(2): 72-79.
3 Twarowska-Schmidt, K. and A. Wlochowicz, 1997. Melt-spun asymmetric poly(4-methyl- 1-pentene) hollow fiber membranes, J. Membr. Sci., 137: 55-61.
4. Desideri, U. and A. Paolucci, 1999. Performance modeling of a carbon dioxide removal system for power plants, Energy Convers. Manage., 40: 1899-1915.
5. Herzog, H., 2001. What future for carbon capture and sequestration? ES&T, 35(7): 148A-153A.
6. Barth, D., C. Tondre, G. Lappai and J. Delpuech, 1981. Kinetic study of carbon dioxide reaction with tertiary amines in aqueous solutions, J. Phys. Chem., 85: 3660-3667.
7. Bird, R.B., W.E. Stewart and E.N. Lightfoot, 1960. Transport Phenomena, JohnWiley & Sons.
8. Blauwhoff, P.M.M., G.F. Versteeg and W.P.M. Van Swaaij, 1984. A study on the reaction between CO_2 and alkanolamines in aqueous solutions, Chem. Eng. Sci., 39: 207-225.
9. Danckwerts, P.V., 1979. The reaction of CO_2 with ethanolamines, Chem. Eng. Sci., 34: 443-446.
10. Happel, J., 1959. Viscous flow relative to arrays of cylinders, AIChE J., 5: 174-177.
11. Liao, C.H. and M.H. Li, 2002. Kinetics of absorption of carbon dioxide into aqueous solutions of monoethanolamine + *N*-methyldiethanolamine, Chem. Eng. Sci., 57: 4569-4582.
12. Reid, R.C., J.M. Prausnitz and B.E. Poling, 1987. The Properties of Gases and Liquids, McGraw-Hill, New York, pp: 577-626.
13. Wang, Y.W., S. Xu, F.D. Otto and A.E. Mather, 1992. Solubility of N_2O in alkanolamines and mixed solvents, J. Chem. Eng., 48: 31-40.
14. Hagewiesche, P.D., S.A. Aami, A. Hani Al-Ghawas and C.S. Orville, 1995. Absorption of carbon dioxide into aqueous blends of monoethanolamine and *N*-methyldiethanolamine, Chem. Eng. Sci., 50: 1071-1079.
15. Hikita, H., S. Asai and T. Takatsuka, 1976. Absorption of carbon dioxide into aqueous sodium hydroxide and sodium carbonate and bicarbonate solutions, Chem. Eng. J., 11: 131-141.
16. Roberts, D. and P.V. Danckwerts, 1967. Kinetics of CO_2 in alkaline solution-I, Chem. Eng. Sci., 17: 961-969.
17. Sharma, M.M. and P.V. Danckwerts, 1966. The absorption of carbon dioxide into solutions of alkalis and amines (with some notes on hydrogen sulphide and carbonyl sulphide), Chem. Eng., pp: CE245-CE280.
18. Vas Bhat, R.D., J.A.M. Kuipers, G.F. Versteeg, 2000. Mass transfer with complex chemical reactions in gas-liquid systems: two-step reversible reactions with unit stoichiometric and kinetic orders, Chem. Eng. J., 76(2): 127-152.
19. Nijsing, R.A.T.O., R.H. Hendriksz, and H. Kramers, 1959. Absorption of CO_2 in jets and falling films of electrolyte solutions, with and without chemical reaction, Chem. Eng. Sci., 10: 88-104.

20. Versteeg, G.F. and W.P.M. Van Swaaij, 1988. Solubility and diffusivity of acid gases (CO_2, N_2O) in aqueous alkanolamine solutions, J. Chem. Eng. Data, 33: 29-34.
21. Weisenberger, S. and A. Schumpe, 1996. Estimation of gas solubility in salt solutions at temperatures from 273K to 363 K, AIChE J., 42(1): 298-300.
22. Ratcliff, G.A. and J.G. Holdcroft, 1963. Diffusivities of gases in aqueous electrolyte solutions, Trans. Inst. Chem. Eng., 41: 315-319.
23. Pohorecki, R. and W. Moniuk, 1988. Kinetics of the reaction between carbon dioxide and hydroxyl ion in aqueous electrolyte solutions, Chem. Eng. Sci., 43: 1677-1684.
24. Tsonopolous, C., D.M. Coulson and L.W. Inman, 1976. Ionization constants of water pollutants, J. Chem. Eng. Data, 21: 190-193.